Homogentisic acid induces aggregation and fibrillation of amyloidogenic proteins

Homogentisic acid induces aggregation and fibrillation of amyloidogenic proteins

Daniela Braconi, Lia Millucci, Andrea Bernini, Ottavia Spiga, Pietro Lupetti, Barbara Marzocchi, Neri Niccolai, Giulia Bernardini, Annalisa Santucci

PII: S0304-4165(16)30446-9
DOI: doi: 10.1016/j.bbagen.2016.11.026
Reference: BBAGEN 28680

To appear in: *BBA - General Subjects*

Received date: 11 May 2016
Revised date: 11 November 2016
Accepted date: 15 November 2016

Please cite this article as: Daniela Braconi, Lia Millucci, Andrea Bernini, Ottavia Spiga, Pietro Lupetti, Barbara Marzocchi, Neri Niccolai, Giulia Bernardini, Annalisa Santucci, Homogentisic acid induces aggregation and fibrillation of amyloidogenic proteins, *BBA - General Subjects* (2016), doi: 10.1016/j.bbagen.2016.11.026

Homogentisic acid induces aggregation and fibrillation of amyloidogenic proteins

Daniela Braconi[1§], Lia Millucci[1§], Andrea Bernini[1], Ottavia Spiga[1], Pietro Lupetti[2], Barbara Marzocchi[1], Neri Niccolai[1], Giulia Bernardini[1§], and Annalisa Santucci[1]*

[1]Dipartimento di Biotecnologie, Chimica e Farmacia, and [2]Dipartimento di Scienze della Vita, Università degli Studi di Siena, 53100, Siena Italy

***Corresponding author at Università degli Studi di Siena - Dipartimento di Biotecnologie, Chimica e Farmacia, via A. Moro 2, 53100 Siena (SI) Italy, Telephone: +39 0577 234958; Fax: +39 0577 234254; E-mail: annalisa.santucci@unisi.it

[§] *These authors contributed equally to this work*

Abbreviations: Alkaptonuria, AKU; Amyloid-A, AA; Atrial Natriuretic Peptide, ANP; Benzoquinone acetate, BQA; Congo Red, CR; High Molecular Weight, HMW; Homogentisate 1,2-dioxygenase, HGD; Homogentisic acid, HGA; Nitro Blue Tetrazolium, NBT; Serum Amyloid A, SAA; Transmission Electron Microscopy, TEM; Transthyretin, Ttr; Western Blot, WB; α-Synuclein, α-Syn.

Keywords: amyloid; Congo Red; gel electrophoresis; inborn error of metabolism; metabolic disease; Serum Amyloid A

ABSTRACT

BACKGROUND: Alkaptonuria (AKU) is an ultra-rare inborn error of metabolism characterized by homogentisic acid (HGA) accumulation due to a deficient activity of the homogentisate 1,2-dioxygenase (HGD) enzyme. This leads to the production of dark pigments that are deposited onto connective tissues, a condition named 'ochronosis' and whose mechanisms are not completely clear. Recently, the potential role of hitherto unidentified proteins in the ochronotic process was hypothesized, and the presence of serum amyloid A (SAA) in alkaptonuric tissues was reported, allowing the classification of AKU as a novel secondary amyloidosis.

METHODS: Gel electrophoresis, Western Blot, Congo Red- based assays and electron microscopy were used to investigate the effects of HGA on the aggregation and fibrillation propensity of amyloidogenic proteins and peptides [Aβ(1-42), transthyretin, atrial natriuretic peptide, α-synuclein and SAA]. LC/MS and *in silico* analyses were undertaken to identify possible binding sites for HGA (or its oxidative metabolite, a benzoquinone acetate or BQA) in SAA.

RESULTS: We found that HGA might act as an amyloid aggregation enhancer *in vitro* for all the tested proteins and peptides in a time- and dose- dependent fashion, and identified a small crevice at the interface between two HGD subunits as a candidate binding site for HGA/BQA.

CONCLUSIONS: HGA might be an important amyloid co- component playing significant roles in AKU amyloidosis.

GENERAL SIGNIFICANCE: Our results provide a possible explanation for the clinically verified onset of amyloidotic processes in AKU and might lay the basis to setup proper pharmacological approaches to alkaptonuric ochronosis, which are still lacking.

1. INTRODUCTION

Alkaptonuria (AKU) (OMIM: 203500) is an ultra-rare inborn error of metabolism whose morbidity is due to gene mutations leading to a defective homogentisate 1,2-dioxygenase (HGD) (E.C.1.13.11.5), an enzyme involved in the catabolic pathway of the aromatic aminoacids phenylalanine and tyrosine. Such a defect causes the inability to metabolize homogentisic acid (HGA) into maleylacetoacetic acid. HGA levels in serum of AKU patients can vary greatly due to dietary intake of phenylalanine and tyrosine, and are reported to range from 5.8 to 400 µmol/l [1-4]. Excess HGA is partly excreted with urine and partly accumulated in connective tissues as a pigmented polymer, a phenomenon known as 'ochronosis' that is the hallmark of AKU. Due to the presence of the ochronotic pigment in a number of tissues/organs, AKU patients undergo a premature and disabling form of severe arthritis-like joint damage (ochronotic arthropathy) and often develop aortic valve and coronary artery disease. Other organs may be also severely affected by ochronosis. No licensed treatment is still available for AKU.

Numerous lines of evidence indicate that the production of the ochronotic pigment is a process involving both the oxidation of HGA into benzoquinone acetate (BQA) with production of ROS, and its consequent polymerization [5, 6]. The relevance of HGA-induced oxidative stress in AKU ochronosis is now well established [7-14]. The interaction of BQA with serum proteins has been proven as well [11]. Importantly, it was recently demonstrated that AKU is associated to a secondary amyloid-A (AA) amyloidosis, and experimental evidence that AA-amyloid deposits are present in different tissues and organs of AKU patients was provided [8, 15-17]. The co-localization of ochronotic pigment and AA-amyloid was highlighted [7-9, 15-20]. Serum Amyloid A (SAA) release, amyloid production and ochronosis were found in HGA-treated human cells [20] and in AKU chondrocytes [19]. Chronic inflammation has long been recognized as central to the induction of AA amyloidosis: a chronic inflammatory status of AKU patients was proven by their high SAA plasma levels [8, 15-18] and pro-inflammatory cytokines [8, 20]. Co-localization of lipid peroxidation and amyloidosis was reported and positively correlated to the presence of ochronotic pigment as well [8, 17]. Aberrant expression of proteins involved in amyloidogenesis, folding and proteases was also found in AKU cells concomitantly with protein oxidation/aggregation [7, 9, 10].

Basing on the above lines of evidence, in the present work we investigated if HGA and its oxidised forms could have an active role in inducing protein amyloidogenic aggregation. Such an ability of HGA was tested with well-known amyloidogenic proteins/peptides, such as: i) Aβ(1-42) peptide, involved in Alzheimer's disease; ii) Transthyretin (Ttr), involved transthyretin-related hereditary amyloidosis; iii) Atrial Natriuretic Peptide (ANP), responsible for isolated atrial amyloidosis; iv) α-synuclein (α-Syn), etiological agent of Parkinson's disease; v) SAA, responsible for AA-amyloidosis. In particular, Aβ(1-42), ANP and Ttr were first used as aggregation-prone models. Then, moving on from this set of data, more in depth analyses were carried out only in α-Syn and, due to its relevance in AKU-related amyloidosis, in SAA.

In all the tested models, HGA (the only perturbing agent applied) significantly accelerated *in vitro* aggregation leading to the production of oligomers, high molecular weight (HMW) aggregates, protofibrils and fibrils. BQA binding to SAA and α-Syn was also demonstrated for the first time, and an *in silico* simulation of HGA-induced unfolding and aggregation was provided based on experimental data.

2. MATERIAL AND METHODS

2.1. Proteins and peptides

One mg of ANP (AnanSpec Inc. San Jose CA, USA) was dissolved in H_2O pH 7.4 (1 ml) and centrifuged at 16,500 × g for 1 hour. The supernatant was collected and filtered (20 nm). Protein concentration was determined at 280 nm and brought to 1µg/10µl.

Fifty µg of Aβ(1-42) peptide (H-1368 Bachem, Bubendorf, S) were first reduced to monomer [21, 22] then solubilised in 500 µl PBS (10 mM, pH 7.4).

Five hundred µg of lyophilized Ttr from human plasma (P1742 Sigma-Aldrich, Milan, IT) were dissolved in 200 µl acetate buffer (100 mM pH 4.0) according to [23] and filtered (0.22 µm) (final concentration 2.5 µg/µl).

Fifty µg of human recombinant SAA (SRP4324 Sigma-Aldrich) were solubilised according to manufacturer's protocol and to previously published papers [24, 25] with minor modifications.

Briefly, SAA was dissolved in 50 µl 0.1% (v/v) acetic acid, then diluted by adding 20 mM HEPES (pH 7.4) to reach 1 µg/10 µl as final concentration and filtered (0.22 µm).

Five hundred µg of human recombinant α-Syn (S7820 Sigma-Aldrich) were dissolved in 200 µl of 20 mm Tris-HCl (pH 7.4) and filtered (0.22 µm) obtaining a final concentration of 2.5 µg/µL similarly to previously published papers [26, 27].

All the above described protein/peptide solutions were split into four different aliquots, one left untreated (control) and the others treated with 0.66 mM, 0.33 mM and 0.165 mM HGA, respectively (additions made by using a 10 mM HGA stock solution prepared freshly in the corresponding buffer). The two lower concentrations were included to fall in the range of HGA levels in AKU patients' serum [4]. In parallel, blank devoid of proteins/peptides were prepared as well. All samples, controls and blanks were incubated at 37°C. Aliquots were taken immediately after HGA addition (time zero) and at several time points during incubation. Aliquots were used immediately for all the assays except for SDS-PAGE analysis, for which they were all previously stored at -32°C in Laemmli sample buffer.

For additional experiments, aliquots from both control and HGA-treated SAA samples at 14 days incubation were briefly centrifuged to remove the supernatant (11,000 rpm, 5 min at room temperature) and resuspended in an equal volume of freshly prepared buffer with 0.33 mM HGA. All the samples were then incubated at 37°C for additional 14 days before being submitted to Congo Red (CR) staining and TEM.

2.2. Spectrophotometric CR binding assay

A 100–300 mM CR (Sigma-Aldrich) stock solution was prepared in filtered PBS (pH 7.4) containing 10% ethanol. Ethanol was added to prevent CR micelle formation. The solution was filtered three times using Gelman extra-thick glass fiber filters (0.3 µm nominal pore retention) and concentration was checked by measuring the absorbance at 505 nm. CR–binding studies were carried out using a protocol modified from Klunk et al. [28]. The test samples were mixed with the PBS-CR solution to yield a final CR concentration of 20 µM. The freshly prepared mixtures of CR and proteins/peptides were incubated at room temperature for 15 min prior to spectral analysis. Control samples containing only CR (without protein) and only the aggregated protein test sample (without CR) were prepared in parallel. Appropriate blanks were prepared and used to rule out any possible interference. Spectrophotometric analysis of CR binding was performed using an Agilent 8453 spectrophotometer (Agilent Technologies, Cernusco sul Naviglio, Milan, IT); all measurements were taken in wavelength-scanning mode (300–700 nm) with the instrument blanked on PBS; absorbance at 541 nm was recorded.

2.3. CR staining

Aliquots (5 µl) of HGA-treated samples and controls were deposited onto slides and let dry for 15 minutes at 37°C, then they were incubated in 20 µM CR in 20% (v/v) ethanol and observed under a polarized light microscope (Zeiss Axio Lab.A1, Arese, Milano). In parallel, bright field images were acquired as well.

2.4. SDS-PAGE and Western Blot (WB)

18% Tricine SDS-PAGE followed by silver staining was used for Aβ(1-42). SDS-PAGE followed by WB was used in the analysis of the HGA-induced aggregation of SAA, Ttr and α-Syn. SDS-PAGE was carried out on 12% precast gels (Bio-Rad, Milan, Italy). Only in the case of Ttr, in order not to dissociate tetramer structures according to [23], samples were dissolved in Laemmli sample buffer avoiding the heating step prior to loading. After SDS-PAGE, proteins were electroblotted onto nitrocellulose membranes.

For WB analysis, the following primary antibodies were used 1:200 with overnight incubations: rabbit polyclonal IgG SAA antibody (sc-20651, Santa Cruz Biotechnology, Dallas, Texas, USA); mouse monoclonal IgG1 α-Syn antibody (3G282, Santa Cruz Biotechnology); rabbit polyclonal IgG Ttr antibody (sc-13098, Santa Cruz Biotechnology). Appropriately diluted secondary HRP-conjugated antibodies were adopted (2 hours at room temperature) and revelation was achieved by a chemiluminescence reaction using the Immun-star™ HRP kit (Bio-Rad).

2.5. NitroBlue Tetrazolium (NBT) staining

In the case of SAA and α-Syn, NBT staining for quinoproteins was performed by incubating nitrocellulose membranes with 0.24 mM NBT (Sigma-Aldrich) in 2 M potassium glycinate (pH 10.0) for 45 min in the dark and washing in 0.1 M sodium tetraborate (pH 10.0) [29].

2.6. Image acquisition and analysis

Chemilumiscence signals were acquired with ImageQuant LAS 4000 (GE Healthcare Life Sciences, Milan, IT). Images of silver stained gels and NBT-stained nitrocellulose membranes were acquired with Image Scanner (GE Healthcare Life Sciences). Quali-quantitative analysis of bands was performed with Imagequant TL software (GE Healthcare Life Sciences). The % volume of each detected band within single lanes was calculated to allow comparison of samples.

2.7. Statistical analysis

All of the experiments were performed in triplicate, showing good reproducibility. Independent sample *t*-test was used to evaluate statistical differences between HGA-treated samples and controls. At least a P value$\leq$0.05 was considered significant.

2.8. Negative staining Transmission Electron Microscopy (TEM)

A 3.5 µl drop of protein suspension was applied to a 300-mesh grid coated with a thin carbon film supported by formvar film. The solution was allowed to sediment on grids for 1 min, then most of it was blotted away with filter paper before adding 3.5 µl of 1% (w/v) aqueous uranyl acetate solution. After 30 seconds of incubation in wet chamber, the solution was blotted away and grids were air dried before observation. Conventional dose images of negatively stained specimens were recorded at variable magnification using a FEI Tecnai G2 Spirit transmission electron microscope operating at 100 kV.

2.9. LC/MS

Possible binding sites for BQA to SAA were investigated by means of LC/MS. Aliquots of control (untreated) and HGA-treated (0.33 mM) SAA prepared as described previously (25 µl) were digested overnight @ 37°C each with 0.2 µg mass spectrometry grade trypsin (Trypsin Gold MS, Promega, Madison, WI, USA according to manufacturer's instructions. Samples were then analysed with HPLC Dionex UltiMate(tm) 3000 (Dionex, Sunnyvale, CA, USA) coupled with LTQ-Orbitrap (Thermo Fisher Scientific Inc. Waltham, MA, USA). Chromatographic separation was carried out with an Acclaim® PepMap100 C18 column (5 µm particle size, 100 Å pore size, 300 µm×150 mm) (Thermo Fisher Scientific Inc.) kept @ 30°C using a 20 µl injection volume (4 µl/min). The LC mobile phase were 0.1% formic acid in water (A) and 0.1% formic acid in acetonitrile (B). MS data were collected using positive electrospray ionization [sheat gas pressure(N_2) 20 (arbitrary units), auxiliary gas pressure 5 (arbitrary units) spray voltage 4.5 kV, capillary temperature 230°C, capillary voltage 49 V and tube lens 185 V] over a range mass of 500 - 2000 m/z in data dependent scan mode with high resolution (30000 FWHM). Data were processed with Proteome Discoverer 1.1 software (Thermo Fisher Scientific Inc.).

2.10. Molecular Docking Simulation

The full hexameric structure of human SAA1 protein was reconstructed from the three-dimensional coordinates of the dimeric structure found as asymmetric unit in the Protein Data Bank (PDB ID: 4IP9 [30]) by using PISA software [31]. Molecular docking simulations of HGA and BQA were performed by use of Autodock Vina [32]. Receptor and ligands were prepared for docking runs using of MGLTools utilities [33], while active box and flexible receptor were set-up by use of Pymol (The PyMOL Molecular Graphics System, Version 1.7.0.1 Schrödinger, LLC) and Vina plugin. A 2.2 nm (x), 2.0 nm (y), 2.2 nm (z) box centered on ^{66}GPGG^{69} turn was used, as it was experimentally identified as a possible BQA binding site. Aminoacid side chains that were found both belonging to the box and solvent exposed were set as flexible: F^{24}, E^{27}, S^{40}, F^{86}, Y^{60}, K^{64}, R^{65}. All rotatable bonds of HGA and BQA were set as active. For each ligand, 100 docking runs with large exhaustiveness (64) were performed. For both ligands, a low energy, largely populated cluster (to a 0.2 nm rmsd extent) of docking poses was found.

3. RESULTS

3.1. HGA accelerates aggregation kinetics of amyloidogenic proteins

The interference of HGA in amyloid peptide/protein aggregation kinetics was evaluated spectrophotometrically by monitoring the time-dependent binding of CR dye. ANP, Aβ(1-42), Ttr, α-Syn and SAA were incubated at 37°C in a CR solution containing or not 0.33 mM HGA. We found that HGA promoted the aggregation kinetics of all our *in vitro* models (Figure 1A). Consistently with other reports [34], CR gave a low signal with freshly dissolved untreated (control) and HGA-treated proteins. However, upon incubation, spectrophotometric signal rapidly increased (Figure 1A) resulting in sigmoidal curves. The aggregation process started immediately after sample solubilisation. However, when comparing the aggregation kinetics of untreated and HGA-treated samples,

significantly different profiles were obtained: in all the tested cases the presence of HGA allowed treated samples to completely assembly into amyloid structures able to bind CR within nearly 24 hours (Figure 1A). The absorbance values of HGA-treated samples were always higher respecting to the untreated counterparts.

3.2. HGA induces ochronotic-like discolouration in aggregates of amyloidogenic proteins

Basing on previous observations of ours [11], the development of an HGA-induced ochronotic-like discolouration of buffers and/or precipitates (when visible) was evaluated. All the blanks and samples treated with HGA for Aβ(1-42), SAA and α-Syn developed an ochronotic-like discolouration; this was not the case of Ttr buffer, probably due to the acidic pH of the medium. Though it is known from the literature that alkaline conditions allow the conversion of HGA into BQA, here we have shown, confirming previous observations of ours [11], that even neutral conditions can allow such a process in a reasonable time. A visible precipitate could be found in HGA-treated Aβ(1-42), SAA and α-Syn, as well as in both control and HGA-treated Ttr. Diffuse packs of black ochronotic-like deposits were found during microscopy analysis of HGA-treated Aβ(1-42) and SAA(Figure 1B) together withmassive clumps of scattered pseudo polygonal precipitates (Figure 1C). In the case of SAA, the dark aggregates were found to self-assemble in a lattice-like manner, whereas Aβ(1-42) formed more sparse aggregates, amorphous in shape. Notably, HGA-treated Ttr appeared as a highly ordered aggregated structure compared to its untreated counterpart (Figure 1C).

3.3. HGA induces the production of oligomers and aggregates of amyloidogenic proteins

HGA induced a time and dose-dependent aggregation of the tested amyloidogenic peptides/proteins. For HGA-treated Aβ(1-42), starting from day two, we observed a significant decrease of monomers and increase in HMW aggregates stacked on top of Tricine-SDS PAGE gels compared to the untreated control (Figure 2A and Supplementary Figure 1A). For HGA-treated Ttr, starting from day1, we observed a significant increase in oligomers respecting to the untreated control (Figure 2B and Supplementary Figure 1B).

In the case of α-Syn, differently from what expected, the time zero samplings showed the presence of aggregates even under control conditions, implying that probably α-Syn possess an intrinsic high tendency to aggregate. This finding was also further confirmed by the presence of stacked material at the bottom of each well of SDS-PAGE gel (Figure 3A). After one-day incubation, no significant differences between control and HGA-treated samples could be pointed out, and bands related to α-Syn monomer, dimer and oligomers spread on the upper part of the gel could be visualized. Conversely, after 7 days, increased levels of dimers, oligomers and HMW aggregates were found in HGA-treated samples with respect to the untreated control. Similar results were confirmed after 14 days incubation (Figure 3A). Interestingly, both after 7 and 14 days incubation, a further band of an apparent molecular weight of ≈24 kDa (whose nature is still unknown) could be visualized only in HGA treated α-Syn samples (Figure 3A). Analogously to what we observed in the present work, the interaction process between α-Syn and dopamine derivatives leads to the production of denaturing- and heat-resistant aggregates during the SDS-PAGE analysis [35] that can be found stacked on top of SDS-PAGE gels [36].

SAA, following consistent dose- and time-dependent patterns, underwent a clear HGA induced aggregation. After one-day incubation, SAA dimers and oligomers appeared only in HGA-treated samples. After 7 days, oligomers and HMW aggregates smeared on top of the gels were found only upon HGA treatment whereas only a modest aggregation of SAA, mainly into dimer, could be highlighted under control conditions. A similar aggregation pattern was found after 14 days, when SAA dimers and oligomers progressively disappeared in HGA-treated samples concomitantly with a significant increase in HMW aggregates. Such a massive aggregation was not found under control conditions, where SAA was again mainly detected only as monomer and dimer (Figure 3B).

On such bases, we then moved to investigate if there was a threshold in HGA concentration for which no increased SAA aggregation could be found. SAA was chosen mainly due to its pathological relevance in AKU-related amyloidosis [8, 15, 18, 20]. We challenged SAA for 14 days with HGA concentrations ranging from 80 μM to 10 nM (Figure 3C). These concentrations were chosen to mimic recently reported HGA serum levels in AKU patients [2, 3] and normal subjects (ranging 0.014 – 0.0714 μmol/l) [37]. Further concentrations well-below the threshold of normal subjects were tested as well. A clear time- and dose-dependent HGA-induced SAA aggregation pattern could be found also in this set of experiments (Figure 3C). A precipitate visible to the naked eye appeared in all SAA samples treated with HGA, especially in samples treated with the three highest HGA concentrations (80, 40, 20 μM) (not shown). WB analysis after 1, 7 and 14 days incubation confirmed this tendency as a clear percentage reduction in SAA monomer and an increase in the abundance of dimers, oligomers and HMW aggregates for samples treated with HGA up to one μM

(Figure 3B). Conversely, the aggregation propensity of SAA samples treated with 100 and 10 nM HGA was similar to what found in control conditions. For these reasons, we believe that, at least in our *in vitro* SAA-based model, the lowest HGA concentration able to induce SAA aggregation can be assumed to range between 0.1 and 1 μM, i.e. well below what is found in AKU subjects [2, 3] but nearly in the range of normal subjects [37].

3.4. HGA induces production of amyloid fibres

SAA and α-Syn underwent TEM analysis after 14-days incubation to investigate the nature of the formed aggregates.

In control SAA, amyloid-like fibrils were found (Figure 4A) showing a variety of dimensions and morphologies, including branched ultrastructures with varying degrees of lateral association (Figure 4A a-c). Bundles of fibrils were detected, with an overall diameter ranging approximately 100-150 nm, together with several aggregates. In HGA-treated SAA, many long, mature fibrils were observed, sometimes assembled in thick bundles of laterally coalescent filaments (Figure 4A f). Short worm-like protofibrils were observed and examples of increased elongation of the protofibrillar aggregates were apparent. Overall, HGA-treated SAA was richer than its control in amyloid fibrils, with single straight fibrils uniformly spread out in the sample.

In order to discriminate if HGA could affect the early molecular events in oligomerization and fibril formation or rather have a surface effect onto already preformed fibrils, further TEM analyses were carried out in already aggregated control and HGA-treated SAA samples that were (re)challenged with freshly added HGA. Larger fibrillar, CR birifringent aggregates were found in samples (re)challenged with HGA compared to their HGA-free counterparts, suggesting that the mechanism of HGA action is at least a mixed process (Supplementary Figure 2).

Control α-Syn showed both protofibrils (Figure 4B l-n) and a range of aggregated structures, but no mature amyloid fibril could be observed. HGA-treated α-Syn showed (Figure 4B o-q), numerous aggregates with morphology and size similar to amyloid bundles of protofibrils with different aggregates including spheres and oligomers of associated spheres (diameter 50 nm). In this sample, a dense meshwork of small curvilinear fibrils was observed as well (Figure 4B q).

HGA-treated α-Syn and SAA were both positive to CR staining showing the classic birefringence of amyloid aggregates, while nearly no trace of amyloid was detected in their untreated counterparts (Figure 5). In particular, in the case of SAA, amyloid birefringence in HGA-treated samples was observed lowering HGA concentration up to 5 μM (Figure 5).

3.5. HGA induces the production of BQA-proteins

When analysed for the presence of quinoproteins, both SAA and α-Syn were positive for NBT staining (Figure 6A). Monomeric SAA showed the binding of quinone (BQA)-proteins after seven days of treatment with HGA (each tested concentration) though with a very faint signal (data not shown) which was better visualized after 14 days (Figure 6A). Similar results were obtained with α-Syn, which showed the presence of BQA-SAA monomers and dimers starting from 7 days incubation (Figure 6A). No aspecific staining could be visualized in the time zero samplings nor in control conditions at each sampling both for SAA and α-Syn (Figure 6A).

LC/MS analysis allowed the identification of probable BQA binding sites in SAA. These sites belong to a 21 aminoacid-long fragment spanning from G^{66} to R^{85} residues, whose mass delta between predicted and observed values corresponded to the addition of two BQA molecules (Figure 6B). Two sites were identified as equally probable for the binding of BQA: G^{66} and G^{68} or G^{66} and G^{69} (Figure 6B). Since this fragment was missing in the peptide list obtained during MS analysis of the untreated (control) SAA, we hypothesized that in such a case SAA was aggregated into a structure likely masking this peptide and making it resistant to trypsin digestion. Conversely, the binding of BQA may have induced structural alterations of the aggregated SAA that made this peptide more easily prone to trypsin digestion.

3.6. Analysis of Docking Simulation

Docking simulation of HGA/BQA to the hexameric structure of SAA identified a small crevice at the interface between two subunits as the candidate binding site. The crevice is formed by a pair of alpha-helices 1 belonging to adjacent chains and arranged in a head-to-tail fashion. Due to the hexameric structure, six instances of such crevice are found, showing a triangular arrangement at each end of the SAA central pore (Figure 6C). Notably, the crevice is delimited by the sidechain of R^{47}, which belongs to the nine-arginine charge patch formed by $R^{33}/R^{37}/R^{65}$ from three monomers and surrounding the centre pore. Such residues are critical for glycosaminoglycans (GAGs) binding [30].

On the same side of R^{65}, the crevice is delimited by the N-terminal segment of helix 1 also containing the predicted amylodoigenic peptide ^{20}SFFSFLG^{26} [30], and by the ^{66}GPGG^{69} turn, previously found to bind BQA and preceding the other predicted amylodoigenic peptide ^{70}VWAAEAIS^{77}. Opposite to R^{47}, the binding site is delimited by the C-terminal segment of adjacent helix 1, ^{40}SDMRE^{44}. Docking of HGA and BQA showed equivalent results in terms of i) binding energy and ii) interaction geometry: i) free energy of binding, as calculated in the force field implementation of Autodock Vina, resulted to be -6.8/-6.4 kcal/mol for HGA/BQA, values usually reported as significant (lower than -6.0 kcal/mol) in the Vina universe, especially for such low molecular weight molecules; ii) from Figure 6D is apparent how carboxylic group of the ligands undergoes charge neutralisation by close interaction with R^{65} guanidinium group; the deeply inserted oxydril/carbonyl group is hydrogen bonded to S^{40} sidechain while the opposite one is solvent exposed and interestingly in close distance of G^{66} amide (<0.4 nm). The overall picture given by docking simulation shows HGA/BQA sharing their binding site with other structural determinants of SAA related to amyloidosis, such as amylodoigenic segments and charge patches; in particular the charge neutralisation is known to play a role in SAA dissociation from HDL promoting SAA aggregation [38]. Glycine residues, having a high level of conformational flexibility and a high entropic cost associated with their secondary structure formation, might be strategic in preventing protein aggregation [39]. It is thus tempting to speculate that, potentially, the binding of BQA to glycine residues in SAA might alter such a delicate balance, making the protein more prone to aggregation. Furthermore, such a binding could also alter SAA charge, which is another crucial factor in controlling aggregation [39]. The presence of GAGs, and heparan sulfate in particular, associated to amyloid deposits has been well documented [40-42]. In particular, it has been found that binding of GAGs to murine SAA can have variable effects on its fibrillation [43].

4. DISCUSSION

The present work was undertaken to elucidate at the molecular level the potent activity of HGA as an amyloid aggregation enhancer. We have already shown *in vivo* and *in vitro* that HGA is the first responsible, with its metabolite BQA as the first known effector, for the cell and tissue damage observed in AKU. The rationale for this work is based on previous works of ours showing that HGA could induce alterations of proteins involved in folding/amyloidogenic processes [8, 10] and oxidative stress in a range of *in vitro* and *ex vivo* models [8-14, 20] possibly leading to protein aggregation. Moreover, we previously unequivocally assessed the presence of a secondary amyloidosis in AKU patients, and the coexistence of ochronotic pigment and amyloid deposits in any AKU examined tissue [8, 15-20]. In the present work, we provide new evidence of the important HGA amyloidogenic action, confirming the preliminary role of this metabolite in the development of AKU-associated SAA amyloidosis.

CR spectrophotometric assay, SDS-PAGE and Western Blot, CR staining, TEM microscopy, LC/MS and *in silico* analyses were adopted to evaluate the HGA-mediated induction of *in vitro* amyloid aggregation and the structural alterations of well-known amyloidogenic peptides/proteins. To set-up our *in vitro* experiments, we moved from several lines of evidence linking the ochronotic HGA-induced pigment with amyloid deposits in AKU. Thanks to our preliminary observations in AKU cell and tissue models together with histologic analyses of AKU biopsies, we could infer that HGA could induce alterations of proteins involved in folding/amyloidogenic processes. In the present work, we provide the definitive demonstration of the pro-amyloidogenic action of HGA regardless of the different type of amyloid-prone models tested in this study. Such models are known to mostly form either extracellular [ANP, Aβ(1-42), Ttr and SAA] or intracellular (α-Syn) deposits. In this light, and basing on previous reports on HGD expression, important considerations can be done. Serum HGA levels in AKU range from 5.8 to 400 μmol/l [1-4] while in healthy individuals are almost null [0.014 – 0.0714 μmol/L, according to [37]]. Both HGA and BQA have been classified as low penetrants through blood-brain barrier [44], but HGD expression in brain was found supporting an *in loco* HGA production and accumulation [44]. Similarly, HGD expression was also reported in alkaptonuric cells from the osteoarticular compartment [45] where a local intracellular production and accumulation of SAA was also reported [46]. Consequently, a possible interaction between HGA/BQA and the tested amyloidogenic molecules can be speculated to occur *in vivo* potentially leading to pathological relapses.

It is obvious that the complexity of *in vivo* systems cannot be reproduced *in vitro*; nevertheless, *in vitro* systems were successfully used to elucidate fibrillogenesis at the molecular level,

providing in a reasonable time lapse (*in vivo*, amyloid deposition requires decades) important structural insights onto amyloid formation [41].The major findings of the present investigation can be summarized as follows:

(a) HGA accelerated the rate of amyloid fibril formation in a time- and dose-dependent manner;

(b) amyloidogenic proteins and peptides incubated with HGA showed a faster fibrillization respecting to their untreated counterparts;

(c) HGA maintained fibrillar stability over prolonged periods of time (i.e., 2-week study);

(d) HGA effects on binding and acceleration of amyloid fibril formation could be mediated primarily by BQA binding.

The overall results of this investigation therefore suggest that HGA is an extremely important amyloid co- component that might play significant roles in AKU amyloidosis by binding to amyloid proteins and enhancing amyloid fibril formation. Our results are in good agreement with previous reports on the same peptides/proteins undergone different aggregating stimuli [47-51].

In this study, electron microscopic analysis was performed only at final stages to monitor the possible effects of HGA on amyloid fibril formation, revealing for all the tested proteins the presence of more dense amyloid aggregates (in the form of fibrils or oligomers and protofibrils) when compared to controls. As of today, around forty human diseases have been linked to the conversion of peptides and proteins into fibrillar insoluble aggregates [52]. This is not due to few peculiar aminoacid sequences; rather, it seems a generic feature of polypeptide chains [53]. Aggregation is a complicated process that is likely to involve more than a simple conversion of soluble monomer to fibre. Evidence has recently pointed to the role of soluble amyloid oligomers or prefibrillar aggregation intermediates as the primary toxic species in degenerative amyloid diseases for their plasticity and reactivity towards other molecular targets (differently from the mature amyloid fibrils, which seem to be the inactivated counterparts) [21, 52, 54-59]. Such spherical oligomers, transiently observed, are kinetic intermediates for fibril formation [60]. However, it is not clear yet if they represent obligate intermediates, if they coalesce directly into fibrils [61-63], or rather if they are originated from a non-classical nucleation-dependent fibril assembly pathway [64, 65]. In the case of HGA-amyloid induced aggregation, we can extend the same controversy to the aggregation of many amyloidogenic proteins, since many types of amyloids display the same type of kinetically intermediate, the soluble oligomer, being stable once formed in the presence of HGA. Aβ(1-42), α-Syn and Ttr, oligomers were described as intermediates or precursors of fibril formation, but in our experiments they seem to represent "off pathway" aggregates that populate an alternative aggregation pathway guided by HGA. These observations are coherent with other reports stating that the ability of α-Syn to form α-Syn-dopamine-quinone adducts with oxidized dopamine [66-68], similarly to the BQA action in AKU, and that these adducts block the α-Syn fibrillation and stabilize the potentially most toxic α- Syn oligomers or protofibrils [69, 70]. A better understanding of the mechanism of stabilization of α-Syn fibrillation by catechols and consequently, of amyloid by BQA, is of particular interest for a number of reasons, including an attempt to understand whether the resulting oligomers are toxic.

HGA had a profound effect in maintaining the initial high level of CR binding observed with all the tested amyloid proteins over a 2-week period.

These studies suggest that during incubation of amyloid proteins with HGA, a stable complex is formed that becomes resistant to protease degradation. This postulate is consistent with the results of the present investigation and implicates HGA in the maintenance of amyloid fibril stability. In the present study, the comparison of different amyloid proteins subjected to the HGA action (a) using identical concentrations and conditions that were directly compared in the same experiment and (b) assessing the effects of HGA at different concentration and over a prolonged period of time (2 week), suggested that HGA may be important "seed molecule" or "nucleation factor" for amyloid fibril formation, which ultimately may be essential for the pathogenesis of AKU amyloidogenesis, as observed in the patient's tissues. It is of note that these effects are found even for HGA concentrations proximal to normality. Furthermore, our results should be carefully evaluated in the light of a recent report showing that alkaptonuric brain cells express HGD and can thus produce the ochronotic pigment in loco due to accumulation of HGA, potentially leading to neurological complications [44].

5. CONCLUSIONS

In this work, we provided novel insights into the potential role of HGA as an aggregation enhancer for amyloidogenic peptides/proteins. The HGA-dependent kinetic alterations observed

during the aggregation into amyloid structures suggest the existence of a stochastic process where HGA may promote intermolecular associations. This finding could be further corroborated by *in silico* molecular docking supporting our experimental data and calculating possible conformational HGA/SAA interactions. Similar results of "seeding effects" are typical of other clinical conditions where amyloid can be observed [71, 72]. In conclusion, our findings suggest therefore a role for HGA in the efficiency of nucleation events and a possible explanation for the clinically verified onset of amyloidosis in AKU patients.

Acknowledgements: This work was supported by Telethon Italy grant GGP10058. The authors thank Toscana Life Sciences Orphan_1 project, Fondazione Monte dei Paschi di Siena 2008-2010, and aimAKU – Associazione Italiana Malati di Alcaptonuria (ORPHA263402). The authors also thank Toscana Life Sciences Foundation, Dr. Elisa Vannuccini and Dr. Lorenzo Ghezzi for technical support.

6. REFERENCES

[1] C. Bory, R. Boulieu, C. Chantin and M. Mathieu, Clin Chim Acta 189 (1990) 7-11.
[2] A.T. Hughes, A.M. Milan, A.S. Davison, P. Christensen, G. Ross, J.A. Gallagher, J.J. Dutton and L.R. Ranganath, Ann Clin Biochem 52 (2015) 597-605.
[3] L.R. Ranganath, A.M. Milan, A.T. Hughes, J.J. Dutton, R. Fitzgerald, M.C. Briggs, H. Bygott, E.E. Psarelli, T.F. Cox, J.A. Gallagher, J.C. Jarvis, C. van Kan, A.K. Hall, D. Laan, B. Olsson, J. Szamosi, M. Rudebeck, T. Kullenberg, A. Cronlund, L. Svensson, C. Junestrand, H. Ayoob, O.G. Timmis, N. Sireau, K.H. Le Quan Sang, F. Genovese, D. Braconi, A. Santucci, M. Nemethova, A. Zatkova, J. McCaffrey, P. Christensen, G. Ross, R. Imrich and J. Rovensky, Ann Rheum Dis 75 (2016) 362-7.
[4] A.P. Angeles, R. Badger, H.E. Gruber and J.E. Seegmiller, J Rheumatol 16 (1989) 512-7.
[5] Z.L. Hegedus, Toxicology 145 (2000) 85-101.
[6] Z.L. Hegedus and U. Nayak, Arch Int Physiol Biochim Biophys 102 (1994) 175-81.
[7] D. Braconi, L. Millucci, G. Bernardini and A. Santucci, Free Radic Biol Med 88 (2015) 70-80.
[8] L. Millucci, L. Ghezzi, E. Paccagnini, G. Giorgetti, C. Viti, D. Braconi, M. Laschi, M. Geminiani, P. Soldani, P. Lupetti, M. Orlandini, C. Benvenuti, F. Perfetto, A. Spreafico, G. Bernardini and A. Santucci, Mediators Inflamm 2014 (2014) 258471.
[9] D. Braconi, L. Millucci, L. Ghezzi and A. Santucci, Expert Rev Proteomics 10 (2013) 521-35.
[10] D. Braconi, G. Bernardini, C. Bianchini, M. Laschi, L. Millucci, L. Amato, L. Tinti, T. Serchi, F. Chellini, A. Spreafico and A. Santucci, J Cell Physiol 227 (2012) 3333-43.
[11] D. Braconi, C. Bianchini, G. Bernardini, M. Laschi, L. Millucci, A. Spreafico and A. Santucci, J Inherit Metab Dis 34 (2011) 1163-76.
[12] D. Braconi, M. Laschi, L. Amato, G. Bernardini, L. Millucci, R. Marcolongo, G. Cavallo, A. Spreafico and A. Santucci, Rheumatology (Oxford) 49 (2010) 1975-83.
[13] D. Braconi, M. Laschi, A.M. Taylor, G. Bernardini, A. Spreafico, L. Tinti, J.A. Gallagher and A. Santucci, J Cell Biochem 111 (2010) 922-32.
[14] L. Tinti, A. Spreafico, D. Braconi, L. Millucci, G. Bernardini, F. Chellini, G. Cavallo, E. Selvi, M. Galeazzi, R. Marcolongo, J.A. Gallagher and A. Santucci, J Cell Physiol 225 (2010) 84-91.
[15] L. Millucci, A. Spreafico, L. Tinti, D. Braconi, L. Ghezzi, E. Paccagnini, G. Bernardini, L. Amato, M. Laschi, E. Selvi, M. Galeazzi, A. Mannoni, M. Benucci, P. Lupetti, F. Chellini, M. Orlandini and A. Santucci, Biochim Biophys Acta 1822 (2012) 1682-91.
[16] L. Millucci, L. Ghezzi, G. Bernardini, D. Braconi, P. Lupetti, F. Perfetto, M. Orlandini and A. Santucci, Diagnostic Pathology 9 (2014) 185.
[17] L. Millucci, L. Ghezzi, D. Braconi, M. Laschi, M. Geminiani, L. Amato, M. Orlandini, C. Benvenuti, G. Bernardini and A. Santucci, Int J Cardiol 172 (2014) e121-3.
[18] L. Millucci, D. Braconi, G. Bernardini, P. Lupetti, J. Rovensky, L. Ranganath and A. Santucci, J Inherit Metab Dis 38 (2015) 797-805.
[19] L. Millucci, G. Giorgetti, C. Viti, L. Ghezzi, S. Gambassi, D. Braconi, B. Marzocchi, A. Paffetti, P. Lupetti, G. Bernardini, M. Orlandini and A. Santucci, Journal of Cellular Physiology 230 (2015) 1148-1157.
[20] A. Spreafico, L. Millucci, L. Ghezzi, M. Geminiani, D. Braconi, L. Amato, F. Chellini, B. Frediani, E. Moretti, G. Collodel, G. Bernardini and A. Santucci, Rheumatology (Oxford) 52 (2013) 1667-73.
[21] J. Bieschke, S.J. Siegel, Y. Fu and J.W. Kelly, Biochemistry 47 (2008) 50-9.
[22] C. Ha and C.B. Park, Langmuir 22 (2006) 6977-85.
[23] M.J. Bonifacio, Y. Sakaki and M.J. Saraiva, Biochim Biophys Acta 1316 (1996) 35-42.
[24] Z. Ye, D. Bayron Poueymiroy, J.J. Aguilera, S. Srinivasan, Y. Wang, L.C. Serpell and W. Colon, Biochemistry 50 (2011) 9184-91.
[25] S. Xu, D. Wu, M. Arnsdorf, R. Johnson, G.S. Getz and V.G. Cabana, Biochemistry 44 (2005) 5381-9.
[26] M. Hashimoto, L.J. Hsu, Y. Xia, A. Takeda, A. Sisk, M. Sundsmo and E. Masliah, Neuroreport 10 (1999) 717-21.
[27] N. Pandey, J. Strider, W.C. Nolan, S.X. Yan and J.E. Galvin, Acta Neuropathol 115 (2008) 479-89.
[28] W.E. Klunk, R.F. Jacob and R.P. Mason, Anal Biochem 266 (1999) 66-76.
[29] M.A. Paz, R. Fluckiger, A. Boak, H.M. Kagan and P.M. Gallop, J Biol Chem 266 (1991) 689-92.

[30] J. Lu, Y. Yu, I. Zhu, Y. Cheng and P.D. Sun, Proc Natl Acad Sci U S A 111 (2014) 5189-94.
[31] E. Krissinel and K. Henrick, J Mol Biol 372 (2007) 774-97.
[32] O. Trott and A.J. Olson, J Comput Chem 31 (2010) 455-61.
[33] G.M. Morris, R. Huey, W. Lindstrom, M.F. Sanner, R.K. Belew, D.S. Goodsell and A.J. Olson, J Comput Chem 30 (2009) 2785-91.
[34] V. Zamotin, A. Gharibyan, N.V. Gibanova, M.A. Lavrikova, D.A. Dolgikh, M.P. Kirpichnikov, I.A. Kostanyan and L.A. Morozova-Roche, FEBS Lett 580 (2006) 2451-7.
[35] C.L. Pham, S.L. Leong, F.E. Ali, V.B. Kenche, A.F. Hill, S.L. Gras, K.J. Barnham and R. Cappai, J Mol Biol 387 (2009) 771-85.
[36] W. Xiang, J.C. Schlachetzki, S. Helling, J.C. Bussmann, M. Berlinghof, T.E. Schaffer, K. Marcus, J. Winkler, J. Klucken and C.M. Becker, Mol Cell Neurosci 54 (2013) 71-83.
[37] J.C. Deutsch and C.R. Santhosh-Kumar, J Chromatogr B Biomed Appl 677 (1996) 147-51.
[38] F. Noborn, J.B. Ancsin, W. Ubhayasekera, R. Kisilevsky and J.P. Li, J Biol Chem 287 (2012) 25669-77.
[39] E. Monsellier and F. Chiti, EMBO Rep 8 (2007) 737-42.
[40] J.B. Ancsin, Amyloid 10 (2003) 67-79.
[41] V. Bellotti and F. Chiti, Curr Opin Struct Biol 18 (2008) 771-9.
[42] N. Motamedi-Shad, E. Monsellier, S. Torrassa, A. Relini and F. Chiti, J Biol Chem 284 (2009) 29921-34.
[43] J.J. Aguilera, F. Zhang, J.M. Beaudet, R.J. Linhardt and W. Colon, Biochimie (2014).
[44] G. Bernardini, M. Laschi, M. Geminiani, D. Braconi, E. Vannuccini, P. Lupetti, F. Manetti, L. Millucci and A. Santucci, J Inherit Metab Dis 38 (2015) 807-14.
[45] M. Laschi, L. Tinti, D. Braconi, L. Millucci, L. Ghezzi, L. Amato, E. Selvi, A. Spreafico, G. Bernardini and A. Santucci, J Cell Physiol 227 (2012) 3254-7.
[46] M. Geminiani, S. Gambassi, L. Millucci, P. Lupetti, G. Collodel, L. Mazzi, B. Frediani, D. Braconi, B. Mazzocchi, M. Laschi, G. Bernardini and A. Santucci, J Cell Physiol (in press) (2016).
[47] R. Wetzel, S. Shivaprasad and A.D. Williams, Biochemistry 46 (2007) 1-10.
[48] L. Liu, J. Hou, J. Du, R.S. Chumanov, Q. Xu, Y. Ge, J.A. Johnson and R.M. Murphy, Protein Eng Des Sel 22 (2009) 479-88.
[49] C.D. Borsarelli, L.J. Falomir-Lockhart, V. OstatnÃ¡, J.A. Fauerbach, H.-H. Hsiao, H. Urlaub, E. PaleÄ • ek, E.A. Jares-Erijman and T.M. Jovin, Free Radical Biology and Medicine 53 (2012) 1004-1015.
[50] L. Chen, Y. Wei, X. Wang and R. He, PLoS One 5 (2010) e9052.
[51] M. Shamoto-Nagai, W. Maruyama, Y. Hashizume, M. Yoshida, T. Osawa, P. Riederer and M. Naoi, J Neural Transm 114 (2007) 1559-67.
[52] F. Chiti and C.M. Dobson, Annu Rev Biochem 75 (2006) 333-66.
[53] E. Monsellier, M. Ramazzotti, N. Taddei and F. Chiti, PLoS Comput Biol 4 (2008) e1000199.
[54] A. Relini, S. Torrassa, R. Ferrando, R. Rolandi, S. Campioni, F. Chiti and A. Gliozzi, Biophys J 98 (2010) 1277-84.
[55] G.P. Gellermann, H. Byrnes, A. Striebinger, K. Ullrich, R. Mueller, H. Hillen and S. Barghorn, Neurobiol Dis 30 (2008) 212-20.
[56] B. O'Nuallain, D.B. Freir, A.J. Nicoll, E. Risse, N. Ferguson, C.E. Herron, J. Collinge and D.M. Walsh, J Neurosci 30 (2010) 14411-9.
[57] B. Caughey and P.T. Lansbury, Annu Rev Neurosci 26 (2003) 267-98.
[58] R. Kayed, E. Head, J.L. Thompson, T.M. McIntire, S.C. Milton, C.W. Cotman and C.G. Glabe, Science 300 (2003) 486-9.
[59] F. Bemporad and F. Chiti, Chem Biol 19 (2012) 315-27.
[60] M. Necula, R. Kayed, S. Milton and C.G. Glabe, J Biol Chem 282 (2007) 10311-24.
[61] D.M. Walsh, D.M. Hartley, Y. Kusumoto, Y. Fezoui, M.M. Condron, A. Lomakin, G.B. Benedek, D.J. Selkoe and D.B. Teplow, J Biol Chem 274 (1999) 25945-52.
[62] M. Nybo, S.E. Svehag and E. Holm Nielsen, Scand J Immunol 49 (1999) 219-23.
[63] D.M. Walsh, A. Lomakin, G.B. Benedek, M.M. Condron and D.B. Teplow, J Biol Chem 272 (1997) 22364-72.
[64] J.D. Harper, S.S. Wong, C.M. Lieber and P.T. Lansbury, Jr., Biochemistry 38 (1999) 8972-80.
[65] A. Lomakin, D.S. Chung, G.B. Benedek, D.A. Kirschner and D.B. Teplow, Proc Natl Acad Sci U S A 93 (1996) 1125-9.
[66] K.A. Conway, J.C. Rochet, R.M. Bieganski and P.T. Lansbury, Jr., Science 294 (2001) 1346-9.
[67] S.L. Leong, R. Cappai, K.J. Barnham and C.L. Pham, Neurochem Res 34 (2009) 1838-46.
[68] J. Li, M. Zhu, A.B. Manning-Bog, D.A. Di Monte and A.L. Fink, Faseb J 18 (2004) 962-4.
[69] S. Ito, K. Nakaso, K. Imamura, T. Takeshima and K. Nakashima, Neurosci Res 66 (2010) 124-30.

[70] W. Zhou, A. Gallagher, D.P. Hong, C. Long, A.L. Fink and V.N. Uversky, J Mol Biol 388 (2009) 597-610.
[71] S.B. Prusiner, Brain Pathol 8 (1998) 499-513.
[72] K. Lundmark, G.T. Westermark, S. Nystrom, C.L. Murphy, A. Solomon and P. Westermark, Proc Natl Acad Sci U S A 99 (2002) 6979-84.

FIGURE LEGENDS

FIGURE 1. Time-dependent aggregation patterns of Aβ(1-42) (a), Ttr (b), α-Syn (c), SAA (d), ANP (e), in control conditions and after treatment with 0.33 mM HGA (**A**). A visible ochronotic pigmentation was observed after 72 hours in HGA-treated Aβ(1-42) and SAA (magnification 20×) (**B**), and a marked aggregation propensity upon treatment with HGA was observed for Aβ(1-42), Ttr, α-Syn and SAA during microscopy analysis (only representative images are shown) (**C**).

FIGURE 2. Analysis of HGA-induced aggregation. Tricine SDS-PAGE and silver staining (images in Supplementary Figure 1A) were used to evaluate the presence of Aβ(1-42) monomer, dimer, oligomers and HMW aggregates up to 6 days incubation @ 37°C in 10 mM PBS pH 7.4 with 0.33 or 0.165 mM HGA and in control conditions (untreated) (**A**). SDS-PAGE and Western Blot (images in Supplementary Figure 1B) were used to evaluate the presence of Ttr monomer, dimer, and oligomers up to 5 days incubation @ 37°C in 100 mM acetate buffer (pH 4.0) with 0.66, 0.33 or 0.165 mM HGA and in control conditions (untreated) (**B**). A quali- quantitative analysis was performed on % volume of each detected band within each single lane to compare controls and HGA- treated samples. Average values ± standard deviation are reported; * denotes statistically significant differences between HGA-treated samples and controls (fold-change *vs.* control ≥2.0).

FIGURE 3. Analysis of HGA-induced aggregation of α-Syn up to 14 days incubation at 37°C in 20 mM Tris-HCl buffer (pH 7.4) with 0.165, 0.33 or 0.66 mM HGA and in control conditions (untreated) was carried out by means of SDS-PAGE and Western Blotting (mouse monoclonal IgG1 α-Syn antibody) (**A**). Analysis of HGA-induced aggregation of SAA up to 14 days incubation @ 37°C in 0.01% (v/v) acetic acid in 20 mM HEPES (pH 7.4) was carried out by means of SDS-PAGE and Western Blotting (rabbit polyclonal IgG primary SAA antibody, sc-20651 Santa Cruz Biotechnology) (**B**). A wide range of HGA concentrations was tested to find the lowest able to induce aggregation of SAA (**C**). Quali- quantitative analysis was performed on % volume of each detected band within each single lane to compare controls and HGA- treated samples. Average values ± standard deviation are reported; * denotes statistically significant differences between HGA-treated samples and controls (fold-change vs. control ≥2.0).

FIGURE 4. TEM analysis revealed different types of aggregates in untreated SAA, including thin flexible protofibrils (**A**, a) and rigid fibrils of various widths (**A**, b and c). In SAA treated with 0.33 mM HGA, thin flexible protofibrils (**A**, d and e) and rigid fibrils (**A**, d-i) were found as well but they were quantitatively more abundant and often forming bundles of longer and bigger coalescent fibres (**A**, e). Rigid fibrils were mostly narrow (nearly 4-5 nm wide) and straight, though they also sometime appeared twisted and thicker (10-20 nm wide). Cluster of thin protofibrils assembled into a lattice like structure were found. Control α-Syn contained a combination of amorphous aggregates and thin, little flexible fibrils creating a dense twist (**B**, l-n). In 0.33 mM HGA-treated α-Syn both short, disordered, fibrillar aggregates and bundles of clumped proto-fibrils associated in irregular clusters were observed (**B**, o-q). An increased proportion of short pre-fibrillar structures and aggregated material was present in this sample (**B**, q).

FIGURE 5. Birefringence of amyloid aggregates formed by SAA and α-Syn upon treatment with HGA (14 days incubation, HGA concentration shown in panels).

FIGURE 6. Clear purple band that were clues for the binding of BQA were visible after NBT-staining in correspondence to α-Syn monomer and dimer (**A**, arrows, left panel) and SAA monomer (**A**, arrows, right panel) after incubation in presence of HGA. LC/MS was used to identify possible sites of BQA binding to SAA, which were found in correspondence to G^{66} and Gly^{68}, and G^{66} and Gly^{69} (**B**). In silico analyses of the SAA hexamer structure was used to study possible HGA/BQA interaction with SAA (an image of SAA as viewed down the central pore axis is presented in **C**, left panel). The nine-arginine charge patch formed by $R^{33}/R^{37}/R^{65}$ of three monomers is coloured in blue, while other colours represents the different subunits. HGA/BQA are represented as yellow spheres bound to the crevices found at monomer/monomer interface in a triangular arrangement around the charge patch. In panel **D**, two adjacent monomers are represented as green and cyan ribbons, with their respective helix 1 labelled, while the $^{66}GPGG^{69}$ turn is labelled by residue and represented as sticks. The pair of helices 1 forms the crevice where the HGA/BQA are docked; main interactions with R^{47} and S^{22} are displayed as dashed lines, while closeness to G^{48} is apparent. Peptides predicted as amylodoigenic and spanning residue 20-26 and 70-77 are also reported in yellow.

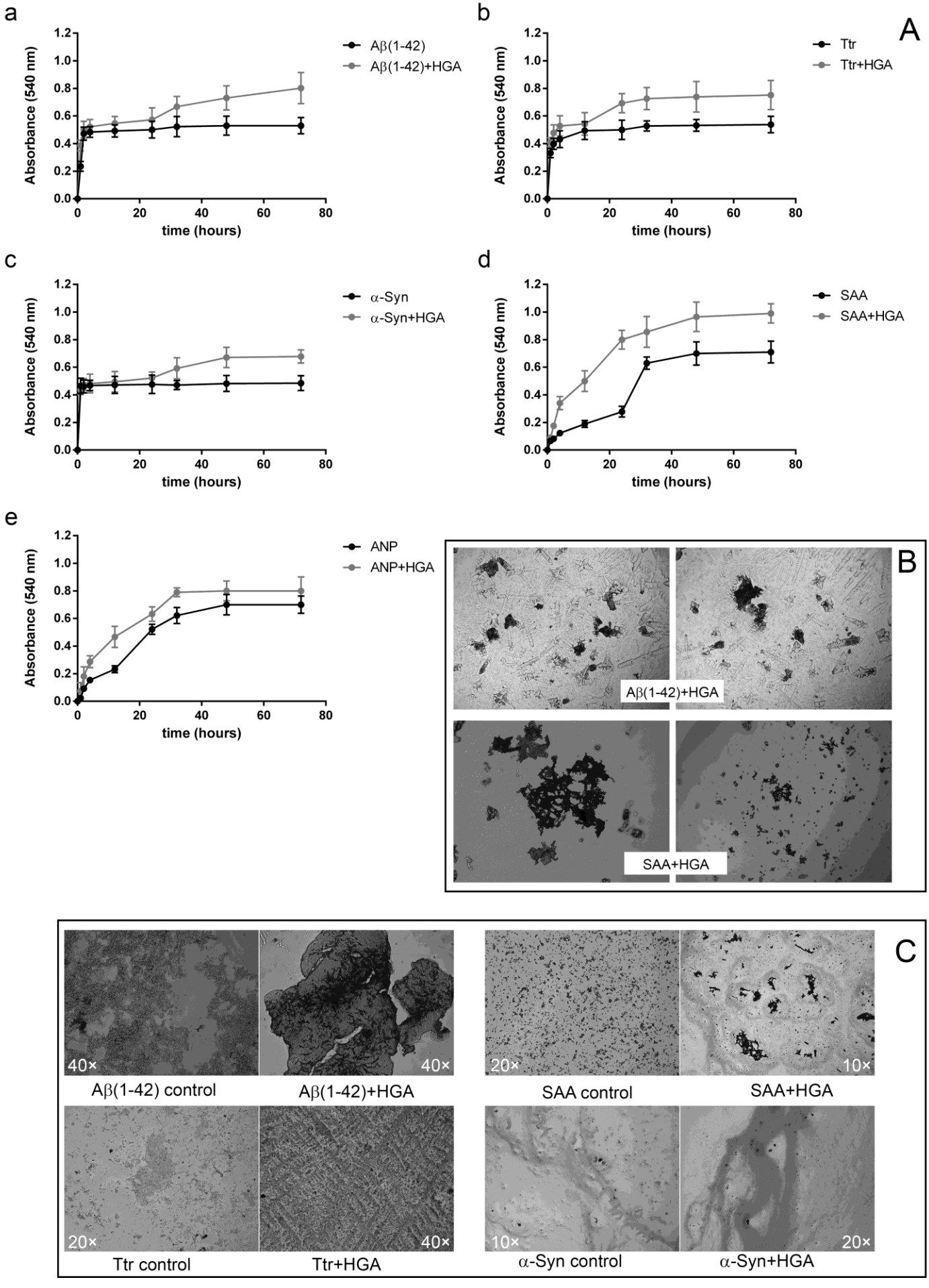
A
a
Absorbance (540 nm)
time (hours)
Aβ(1-42)
Aβ(1-42)+HGA
b
Ttr
Ttr+HGA
c
α-Syn
α-Syn+HGA
d
SAA
SAA+HGA
e
ANP
ANP+HGA
B
Aβ(1-42)+HGA
SAA+HGA
C
40×
Aβ(1-42) control
Aβ(1-42)+HGA
20×
SAA control
10×
SAA+HGA
Ttr control
Ttr+HGA
α-Syn control
α-Syn+HGA

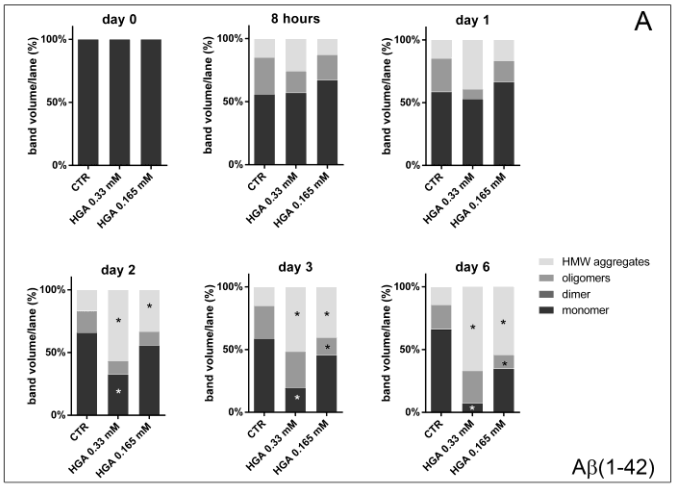

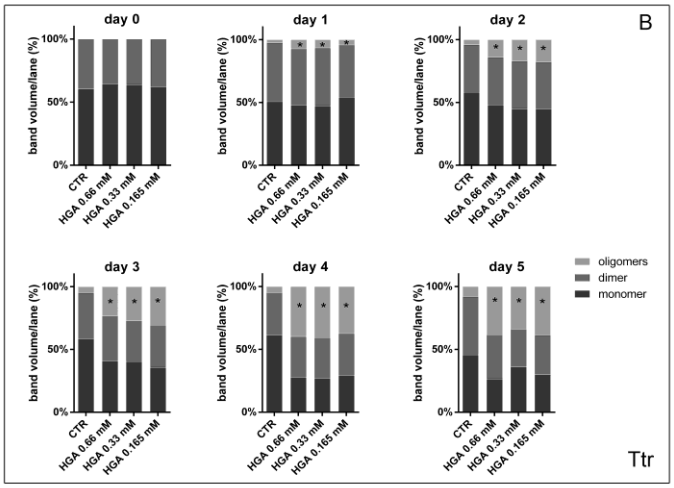

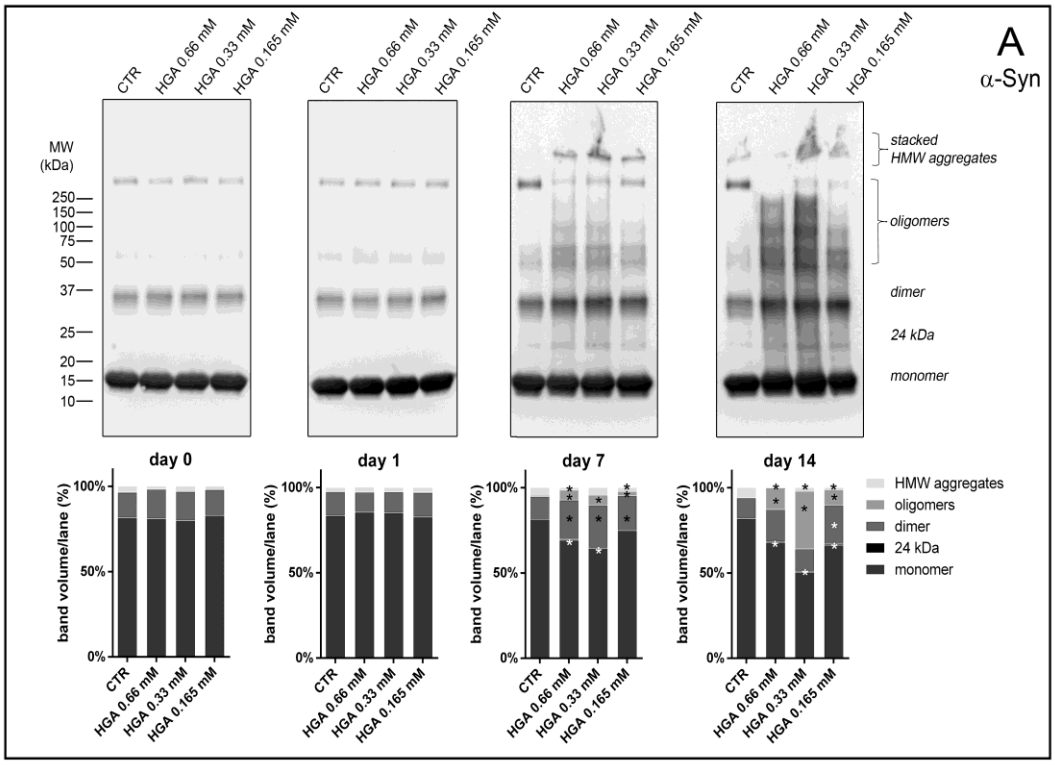
A
α-Syn
CTR
HGA 0.66 mM
HGA 0.33 mM
HGA 0.165 mM
MW (kDa)
250
150
100
75
50
37
25
20
15
10
stacked HMW aggregates
oligomers
dimer
24 kDa
monomer
day 0
day 1
day 7
day 14
band volume/lane (%)
100%
50%
0%
HMW aggregates
oligomers
dimer
24 kDa
monomer

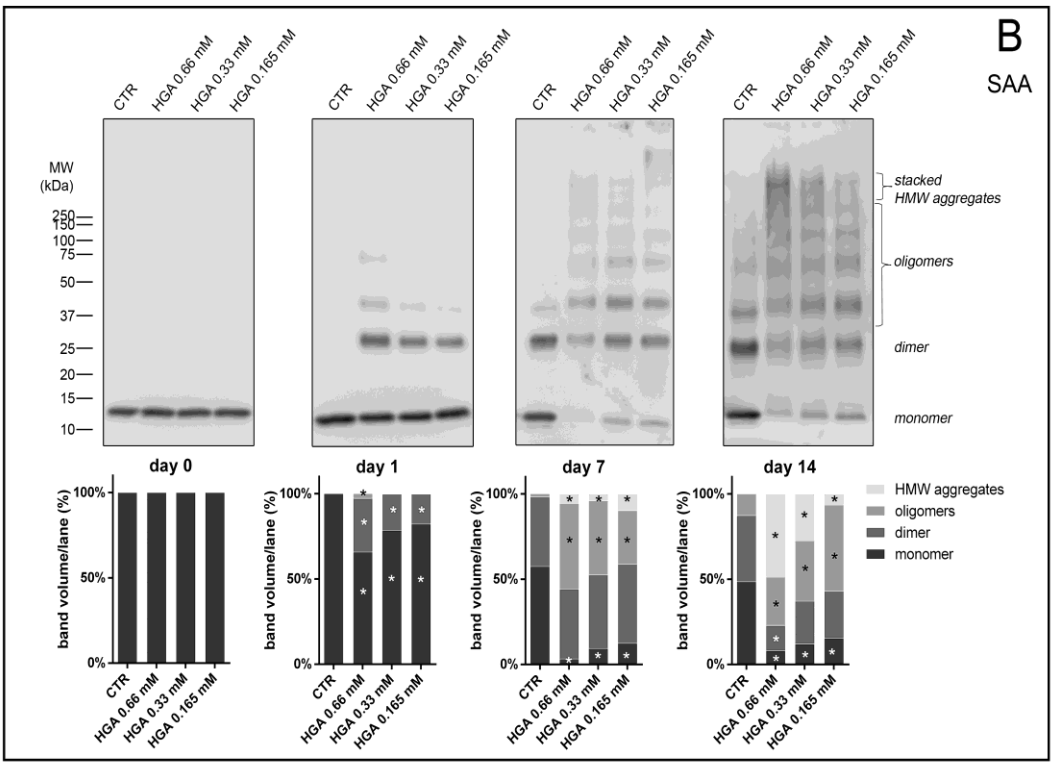
B
SAA
CTR
HGA 0.66 mM
HGA 0.33 mM
HGA 0.165 mM
MW (kDa)
250
150
100
75
50
37
25
20
15
10
stacked HMW aggregates
oligomers
dimer
monomer
day 0
day 1
day 7
day 14
band volume/lane (%)
100%
50%
0%
HMW aggregates
oligomers
dimer
monomer

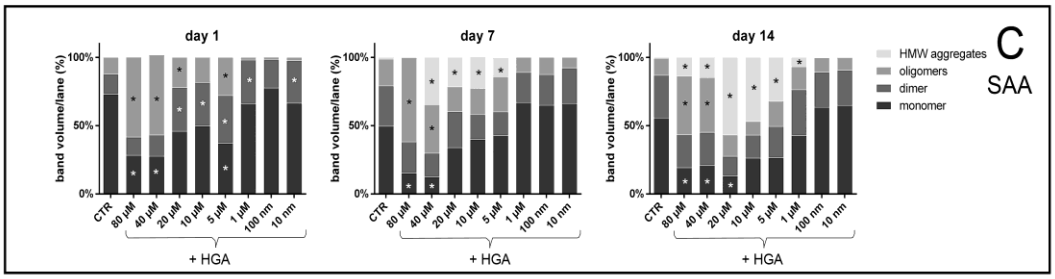
C
SAA
day 1
day 7
day 14
band volume/lane (%)
100%
50%
0%
CTR
80 µM
40 µM
20 µM
10 µM
5 µM
1 µM
100 nM
10 nM
+ HGA
HMW aggregates
oligomers
dimer
monomer

Figure 1

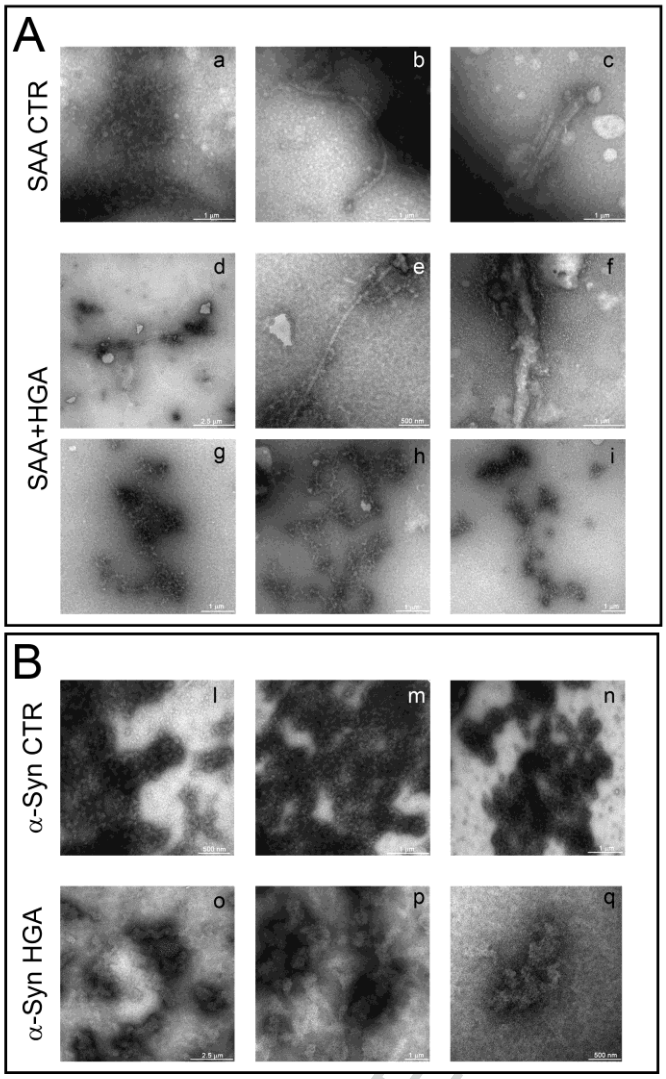

Figure 2

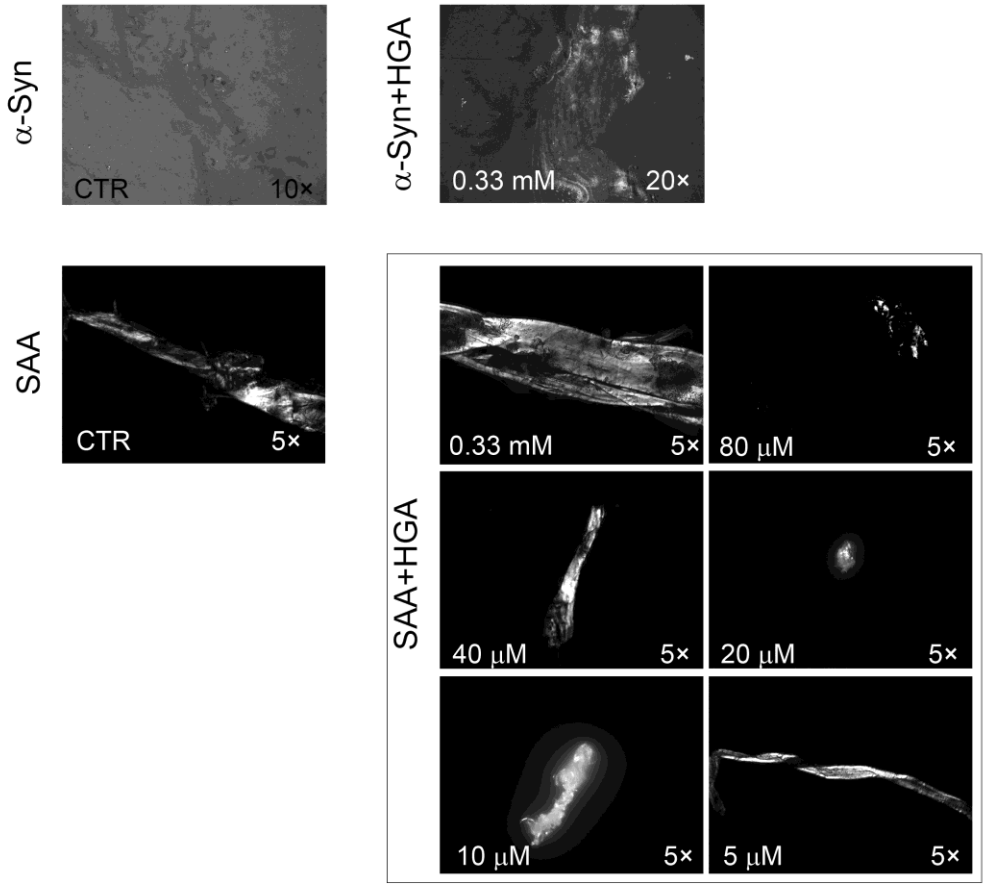

Figure 3

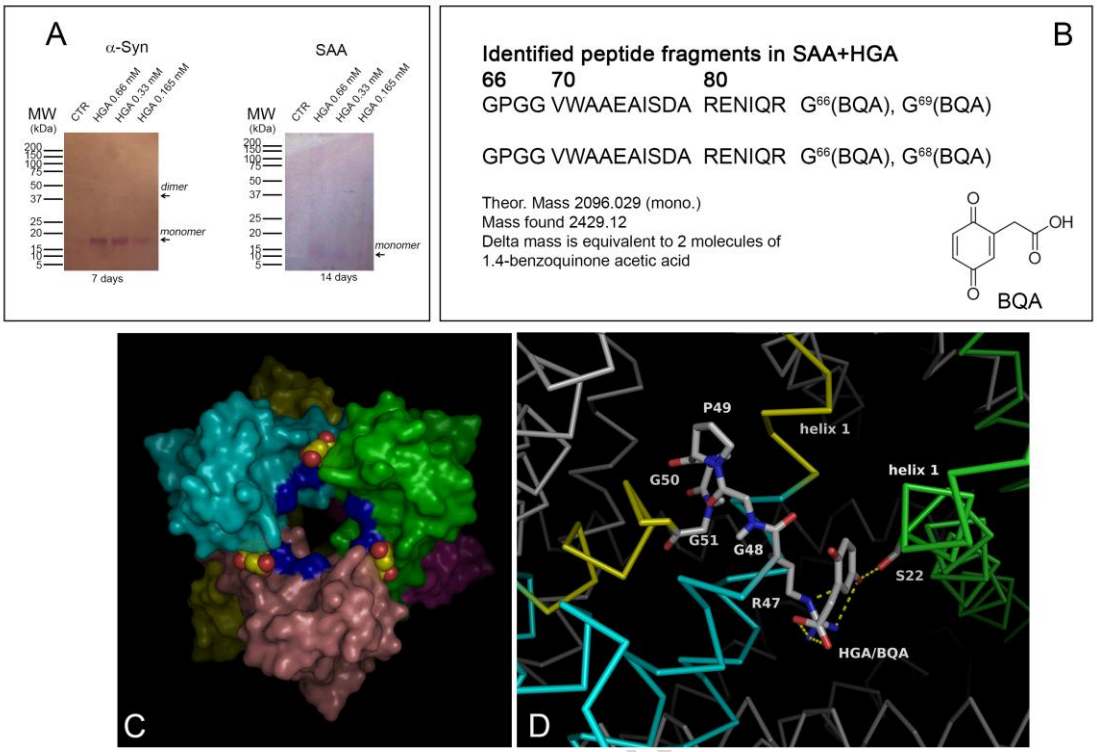

Figure 4

Homogentisic acid induces aggregation and fibrillation of amyloidogenic proteins

Daniela Braconi[1§], Lia Millucci[1§], Andrea Bernini[1], Ottavia Spiga[1], Pietro Lupetti[2], Barbara Marzocchi[1], Neri Niccolai[1], Giulia Bernardini[1§], and Annalisa Santucci[1]*

[1]Dipartimento di Biotecnologie, Chimica e Farmacia, and [2]Dipartimento di Scienze della Vita, Università degli Studi di Siena, 53100, Siena Italy

Highlights

- HGA promotes the aggregation kinetics of amyloidogenic peptides/proteins
- HGA enhances the aggregation into different amyloid structures
- BQA, originated from oxidation of HGA, can bind to SAA and α-Syn
- LC/MS and *in silico* analyses indicate possible binding sites for HGA and BQA in SAA